Inorganic Chemistry

Article

pubs.acs.org/IC

Direct Synthesis of High-Quality Water-Soluble CdTe:Zn^{2+} Quantum Dots

Qisui Wang,[†,‡] Tingting Fang,[†] Peng Liu,*[,†] Bohua Deng,[†] Xinmin Min,[†,‡] and Xi Li[†]

[†]Department of Chemistry, School of Sciences, Wuhan University of Technology, Wuhan 430070, P.R. China

[‡]State Key Laboratory of Advanced Technology for Materials Synthesis and Processing, School of Materials Science and Engineering, Wuhan University of Technology, Wuhan 430070, People's Republic of China

ABSTRACT: The synthesis of water-soluble and low-cytotoxicity quantum dots (QDs) in aqueous solution has received much attention recently. A one-step and convenient method has been developed for synthesis of water-soluble glutathione (GSH)-capped and Zn^{2+}-doped CdTe QDs via a refluxing route. Because of the addition of Zn ions and the epitaxial growth of a CdS layer, the prepared QDs exhibit superior properties, including strong fluorescence, minimal cytotoxicity, and enhanced biocompatibility. The optical properties of QDs are characterized by UV−vis and fluorescence (FL) spectra. The structure of QDs was verified by transmission electron microscopy (TEM), X-ray diffraction (XRD), X-ray photoelectron spectrometry (XPS), energy dispersive spectroscopy (EDS), atomic absorption spectrometry (AAS), and Fourier transform infrared spectroscopy (FTIR). Furthermore, the low cytotoxicity of the prepared QDs was proved by the microcalorimetric technique and inductively coupled plasma-atomic emission spectrometry (ICP-AES).

INTRODUCTION

II−VI semiconductor nanocrystals (quantum dots (QDs)) represent one of the most important types of nanomaterials. QDs exhibit unique optical properties such as broad absorption, narrow and symmetric emission, high fluorescence quantum yield (QY), high photostability, and particle size-dependent fluorescence (FL), which is characterized by broad excitation ranges and excellent robustness against photobleaching.[1−4]

Synthesis and physical properties of QDs and their applications in various fields have attracted increasing research interests in recent years.[5−14] As an alternative choice to CdSe nanocrystals synthesized in the organic phase, CdTe nanocrystals synthesized in aqueous solution have attracted a lot of research interest.[6,15] This is because CdTe with different sizes can cover almost the whole visible spectral range due to a strong quantum confinement effect and are more suitable for biomedical applications.[6] However, the prepared CdTe QDs ususlly contain the highly toxic heavy-metal element Cd, which raises concerns on safety for biomedical applications. Therefore, some research groups[9,16−19] have prepared ternary alloyed CdTe:Zn^{2+} (or $Zn_{1-x}Cd_xTe$) QDs using ion-doped methods. The ion-doped QDs can greatly reduce the ratio of toxic Cd in QDs and thus improve their applicability in biological studies.[20] The photostability, thermostability, and QY have also been improved.[20] Usually, the ternary alloyed QDs are synthesized and mentioned above through a classic organometallic or multistep aqueous phase synthesis method. The synthesis of $Zn_{1-x}Cd_xTe$ nanocrystals using organometallic method requests high synthesis temperature and toxic chemical reagents. The prepared ternary alloyed QDs with the aqueous phase method require at least two steps: the synthesis of Te precursor and the growth of QDs. As we know, the preparation method of the Te precursor through the chemical reduction of $NaBH_4$ and Te powder is not convenient and time-consuming. In this method, the Te precursor is susceptible to oxidation, and the reaction must be stored in a dry and oxygen-free environment. As in some other reports,[21] H_2Te was used as a source of Te precursor, which is a highly toxic and flammable gas. Thus, it is of great significance to develop a strategy for one-step synthesis of doped QDs with biocompatibility.

In this paper, we successfully prepared highly fluorescent CdTe:Zn^{2+} QDs by incorporating Zn into CdTe through a one-step aqueous route. Glutathione (GSH) was used as the capping ligand due to its prevalence in most organisms. Furthermore, the cytotoxicity of CdTe:Zn^{2+} QDs was evaluated by a microcalorimetric technique. The obtained QDs will be promising nanomaterials as fluorescent labels for bioapplications.

EXPERIMENTAL SECTION

Chemicals. Cadmium chloride ($CdCl_2$), sodium tellurite (Na_2TeO_3), sodium borohydride ($NaBH_4$), ethanol (C_2H_5OH), sodium hydroxide (NaOH), glutathione (GSH), and other routine chemicals were purchased from Shenshi Chem. Ltd. All the chemicals used were of analytical grade, and double distilled deionized water was used in all experiments.

Synthesis of GSH-Capped CdTe:Zn^{2+} QDs. In a typical synthesis, 22.5 mL of $CdCl_2{\cdot}2.5H_2O$ (2×10^{-2} M) and 2.5 mL of

Received: March 2, 2012
Published: August 16, 2012

   dx.doi.org/10.1021/ic300473u | Inorg. Chem. 2012, 51, 9208−9213

$ZnCl_2$ (2×10^{-2} M) was dissolved in 55 mL of ultrapure water in a 100-mL three-necked flask, and GSH (6×10^{-4} mol), Na_2TeO_3 (10^{-4} mol), and $NaBH_4$ (10^{-4} mol) were added and the pH was adjusted to 10.50 with vigorous stirring. When the solution's color changed to pale green, the mixture was refluxed at 100 °C and different reaction times (0, 5, 10, 20, 30, 50, 60, 80, 100, 130, 160, 190, 220, and 250 min), and GSH-capped CdTe:Zn^{2+} QDs began to grow immediately. To remove the excess GSH−Cd complexes at the end of the synthesis, cold 2-propanol was added to the reaction mixture to precipitate GSH-capped CdTe:Zn^{2+} QDs. The as-prepared product was dried overnight under vacuum at 40 °C for further experiments, or product was dispersed in phosphate buffer solution (pH = 7.2) and stored at 277 K. The preparation of mercaptoacetic acid (MPA) capped CdTe QDs were adopted from the literature.[22]

Characterization. All FL measurements were recorded using a RF-5301 (Shimadzu) fluorometer. The slit widths used for excitation and emission were 5 nm. A Lambda 35 (PerkinElmer) spectrophotometer was used with a cell of 1.0 cm path length. The high-resolution transmission electron microscopy (HRTEM) image of the QDs (CdTe:Zn^{2+} QDs (sample 2), the same below) was acquired on an H-600 (Japan Hitachi) TEM. X-ray diffraction (XRD) patterns were obtained on a D8 Advance X-ray diffractometer (Bruker). X-ray photoelectron spectroscopy (XPS) measurements were acquired with a K-Alpha-surface analysis X-ray photoelectron spectrometer (Thermon Scientific). An energy dispersive spectroscopy (EDS) spectrum was captured using the scanning electron microscope equipped with an energy dispersive X-ray spectrometer (Hitachi, S-4800). The Fourier transform infrared spectra (FTIR) of samples were recorded by FTIR spectroscopy (AVA TAR 370, Thermo Nicolet).

Cytotoxicity Evaluation. Microcalorimetric experiments were performed on a TAM air isothermal microcalorimeter (Thermometric AB, Sweden), which was equipped with eight twin calorimetric channels, of which one side was used for the sample and the other for a static reference.[23−25] The generated signal (metabolic thermogenic) was recorded in situ using a computer. The *Tetrahymena* culture mediums (15 g/L peptone, 5 g/L yeast powder, 1 g/L glucose, pH = 7.2) with a volume of 5 mL were placed in 20 mL glass ampules which had been sterilized. Then different amounts of QDs and *Tetrahymena* suspension were added into each ampule, respectively. After that, the ampules were sealed with a cap and placed into the microcalorimeter, which was controlled at 28 °C by a thermostat. The power-time signals were recorded at an interval of 1 min.

After a month, QDs were precipitated and centrifuged at 10 000 rpm for 10 min. The supernatant was analyzed directly by ICP-AES (TE, IRIS Intrepid II) in order to determine the concentration of Cd^{2+}.

RESULTS AND DISCUSSION

The synthetic process of water-soluble GSH-capped CdTe:Zn^{2+} QDs is described in Figure 1. Compared with other methods,[9,18,19] it is easy to synthesize CdTe:Zn^{2+} QDs with a one-step route.

In order to optimize the synthetic procedure, we studied the influence of different Zn:Cd ratios upon the FL qualities or QY of the prepared QDs in the same reaction. Table 1 shows the

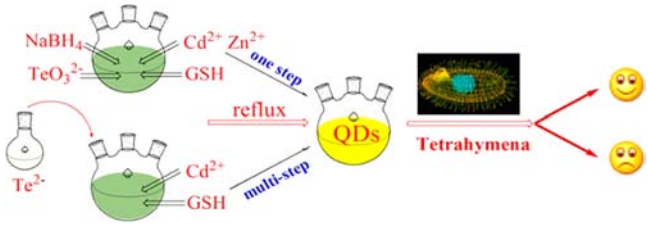

Figure 1. Schematic of the formation of GSH-capped CdTe:Zn^{2+} QDs with one-step synthetic route.

Table 1. Optical Properties of CdTe:Zn^{2+} QDs with Various Chemical Compositions (Reaction Time, 80 min)

sample	Zn/Cd free ratio	Zn/Cd actual composition	FLQY (%)	λ_{abs} (nm)	λ_{em} (nm)
1 (pure CdTe)	0:1	0:1	55	512	561
2	1/10:1	0.085:1	72	508	552
3	1/4:1	0.2:1	65	505	547
4	3/7:1	0.4:1	58	499	544
5	1/2:1	0.44:1	52	493	537
6	1:1	0.87:1	48	490	534
7	2:1	1.7:1	37	471	524

information about the optical properties of QDs with different compositions and the same reaction time of 80 min. The actual constituent ratio of Zn to Cd in the prepared QDs is measured by AAS. With increased Zn ratios, their FLQY were significantly enhanced (samples 2, 3, and 4), and then decreased (samples 5, 6, and 7). The results show that the low addition of Zn^{2+} ions could greatly improve the QY of the QDs and also illustrate the quantity of Zn^{2+} that could influence the quality of QDs. He et al.[19,26,27] proposed that the surface of the QDs may display oxidized Te surface sites which can lead to nonradiative combination pathways, i.e., FL quenching. Thus, the defect sites could be taken by the addition of Zn ions, and then both the QY and stability may be enhanced. Another reason for the improved optical properties of QDs is that the low Zn molar fraction can reduce Cd vacancy defect as the incorporation of Zn into QDs.[9] However, it can be seen from Table 1 that too much Zn^{2+} could not improve the optical properties of QDs. It is because too much Zn molar fraction would increase the Zn-related intrinsic defect in the CdTe:Zn^{2+} QDs structure.[9,28]

Furthermore, Table 1 also shows that the first absorption peak shifted from 512 to 471 nm and the FL emission peak shifted from 561 to 524 nm when the Zn molar fraction increased. The observed systematical blue-shift suggests that the formation of CdTe:Zn^{2+} QDs result from simultaneous reaction of Cd^{2+} and Zn^{2+} with Te ions.[20,29] It is impossible to form separate CdTe and ZnTe quantum dots[29−31] or core−shell structure CdTe/ZnTe.[20,29,31] Because if ZnTe nucleated separately, the corresponding PL and absorption peaks should appear. In addition, if the CdTe/ZnTe core−shell QDs formed, the resulting absorption and FL will shift to longer wavelength as compared with that of pure CdTe due to partial leakage of the exciton into the shell matrix.[29,32] As we know, the XPS method can provide information on the nature and type of constituted elements present on the surface of QDs. Figure 2 shows the XPS spectra of CdTe:Zn^{2+} and CdTe QDs. The appearance of characteristic Zn (2p) peaks at 1019.90 and 1040.30 eV are depicted in the inset of Figure 2, which confirms the presence of Zn in ion-doped QDs.[19] The relative concentrations of Cd and Zn in the CdTe:Zn^{2+} QDs are calculated by dividing the area of XPS signals. The calculated constituent ratio of Zn to Cd is 0.057:1. It is noteworthy that in the alloyed sample the molar ratio of Zn to Cd measured in the XPS signals is less than that of the AAS element analysis result (0.085:1) because XPS is a surface sensitive technique. XPS results also provide further evidence for an alloy structure of the as-prepared QDs.

In order to consider QY, we choose the Zn/Cd feed ratio of 1/10:1 (sample 2) as representative, and the reaction time is from 0 to 250 min. The absorption (a) and FL (b) spectra of a

dx.doi.org/10.1021/ic300473u | Inorg. Chem. 2012, 51, 9208−9213

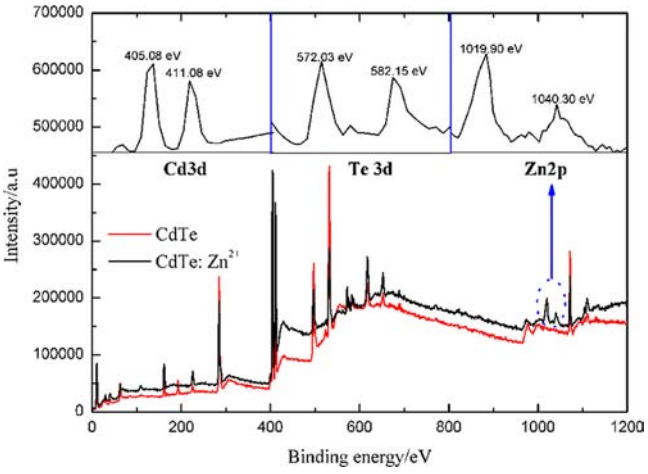

Figure 2. XPS spectra of CdTe:Zn^{2+} QDs and CdTe QDs (sample 2) (the inset are Cd (3d), Te (3d), and Zn (2p) regions).

series of CdTe:Zn^{2+} QDs (sample 2) at different reaction times are presented in Figure 3. It is known that a primary indication

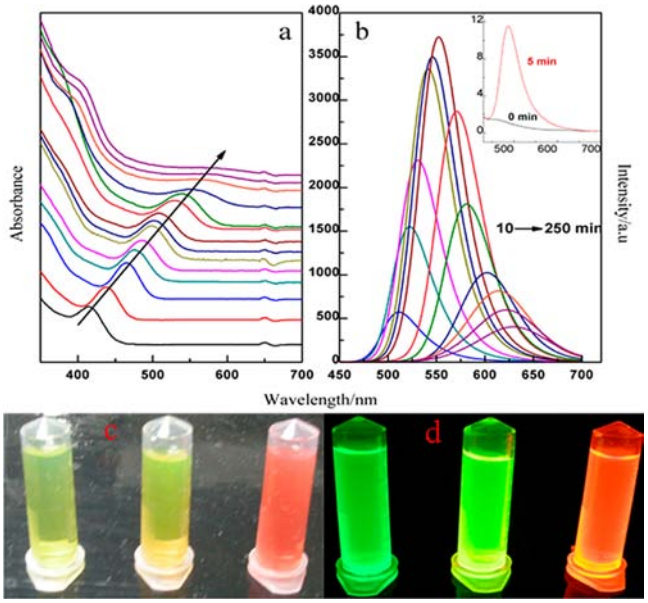

Figure 3. Absorption (a) and fluorescence (b) spectra of CdTe:Zn^{2+} QDs (reaction time, 0−250 min; from left to right; λ_{ex} = 400 nm); photographs of QDs under visible light (c) and 365 nm UV light (d) (reaction time, 10, 80, and 250 min; from left to right).

of the formation of QD particles, compared to bulk species, is a blue shift in the absorbance spectrum.[33] Because quantum confinement effects determine the optical properties of QDs, the degree of electronic confinement is highly correlated with particle size.[34] Figure 3a unambiguously reveals this effect (see the arrow in Figure 3a) and compares the absorption spectra of the QD samples. By controlling the reaction time in the same reaction environment, we obtained different-colored QDs (500−630 nm) as shown in Figure 3b. Photographs of the three samples (10, 80, and 250 min) were taken under visible light and 365 nm UV light, respectively. Figure 3c indicates that the prepared QDs solutions are transparent under visible light, which suggests that these QDs are well-dispersed in aqueous phase without further treatment. Under UV irradiation, the as-prepared QDs solutions emit bright FL as shown in Figure 3d. The FL colors of these alloyed QDs are consistent with the corresponding FL spectra in Figure 3b.

To further understand the above results in our system, XRD, HRTEM, XPS, and EDS were applied to characterize the QDs morphology and structure. The lattice parameters derived from XRD results displayed that the diffraction pattern of the QDs (10 min) was close to that of bulk cubic CdTe (Figure 4),

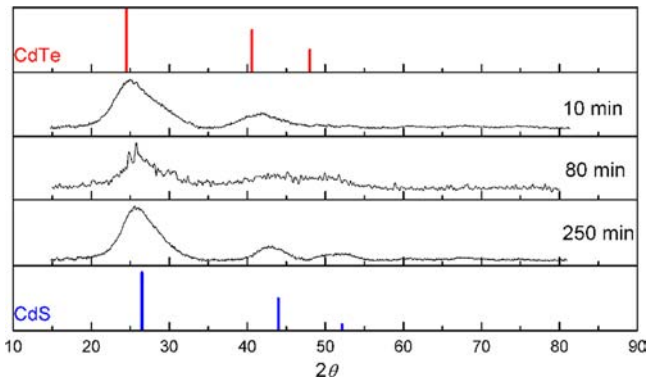

Figure 4. XRD pattern of CdTe:Zn^{2+} QDs.

indicating that its dominant structure was the CdTe crystal phase. In contrast, the diffraction patterns of the QDs (80 and 250 min) gradually shifted to higher angles, which was close to the diffraction peak of pure cubic CdS crystal. This indicates that the CdS shell was slowly formed on the surface of QDs. Furthermore, the molar ratio of Cd^{2+}/Na_2TeO_3/GSH was fixed at 4.5:1:6 in our system. Thus, the surface of CdTe QDs were tightly capped by Cd^{2+}−GSH complex, because the traps which mainly originate from Te atoms with dangling bonds could be occupied by the Cd^{2+}−GSH complex. The Cd^{2+}−GSH complex could form a wall on the surface of the CdTe nanocrystals, rather like ZnS etc. in core/shell nanoparticles. GSH could decompose to give S^{2-} ions over a prolonged reaction time. Sulfur ions would occupy Te positions on the surface of the CdTe core. Thus, CdS and Cd^{2+}−GSH would passivate the CdTe core together. It suggests that GSH not only acts as a stabilizer to bind with Cd^{2+} on the surface of QDs through thiol group (−SH) linkage but also undergoes gradual thermal decomposition to release free S^{2-} to electrostatically interact with Cd^{2+}, forming a CdS shell on the CdTe core.[35,36] So the shell could also greatly improve the QY of the QDs. As a result, this could effectively passivate the surface trap states and prevent the release of Cd^{2+}.

As shown in Figure 5, the well monodispersed CdTe:Zn^{2+} QDs showed average sizes of about 2.5 nm, which is consistent with the results calculated from Peng's formula.[37] The existence of well resolved lattice planes on the HRTEM image further confirms the crystalline structure and high-quality of prepared CdTe:Zn^{2+} QDs. Furthermore, the lattices stretch straight across the QDs with no evidence of an interface, which is consistent with a coherent epitaxial growth mechanism.[36,38−41] Because the lattice mismatch between CdTe and CdS is small, epitaxial growth of CdS on CdTe with very homogeneous crystal structures is obtained, as shown by TEM.

Further evidence on the surface structure of QDs can be obtained from the XPS analysis. An apparent shoulder peak at ~162.23 eV was found after carefully checking the S (2p) XPS spectrum (Figure 6a). Also then the S (2p) peak was

dx.doi.org/10.1021/ic300473u | Inorg. Chem. 2012, 51, 9208−9213

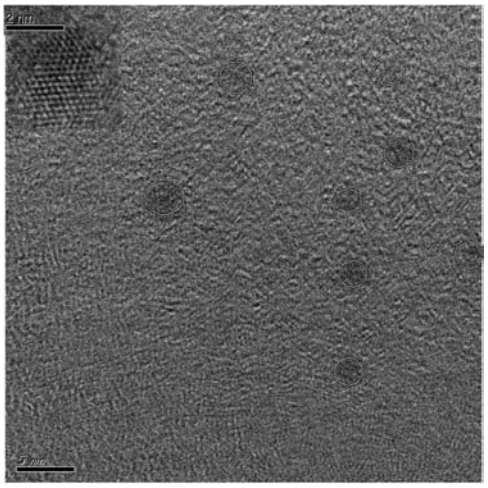

Figure 5. TEM image of CdTe:Zn^{2+} QDs (Zn:Cd = 1/10:1, λ_{em} = 552 nm).

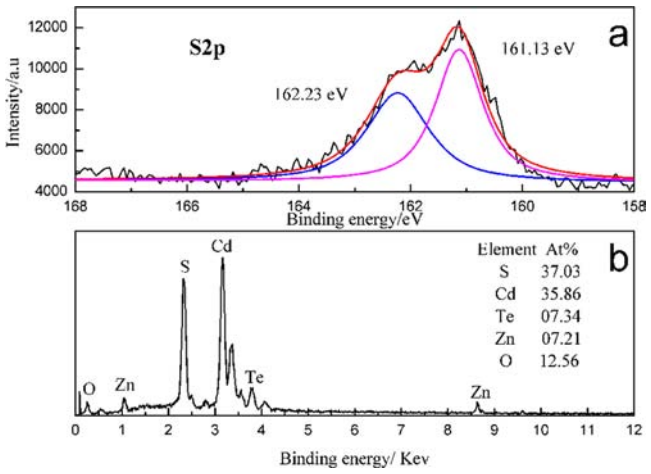

Figure 6. XPS of S2p (a) and EDS (b) spectra recorded from CdTe:Zn^{2+} QDs.

deconvoluted into two separate peaks at 161.13 and 162.23 eV corresponding to the typical characteristic peaks of Cd−S and Cd−SR, respectively.[19,36] The results agree with the conclusion of the XRD spectrum. The EDS technique was also used to probe the surface composition of CdTe:Zn^{2+} QDs. The appearance of characteristic Zn^{2+} peaks are depicted in Figure 6b, which proves the existence of Zn in ion-doped QDs. The ratio of Zn to Cd (about 0.2:1) is more than that of the AAS element analysis result (0.085:1). Because EDS is a semiquantitative characterization tool, it merely exhibits the composition of the QD surface elements. The high ratio of S to Te (5:1) may be attributed to the fact that the GSH ligand together with the CdS shell is attached to the QDs. Thus, the EDS results offer clear evidence of the formation of the CdS shell structure.

To verify the existence of GSH on the surface of the prepared QDs as a stabilizer, we compared the FTIR spectra of free GSH and GSH-capped CdTe:Zn^{2+} QDs. As shown in Figure 7, the IR absorption bands of free GSH at 3127 and 3023 cm^{-1} are ascribed to N−H stretching bands (NH_3^+), whereas the peak at 2526 and 1538 cm^{-1} are assigned to −SH and −NHR groups, respectively. By contrast, the disappearance of the −SH stretching vibrational peak, the almost disappear-

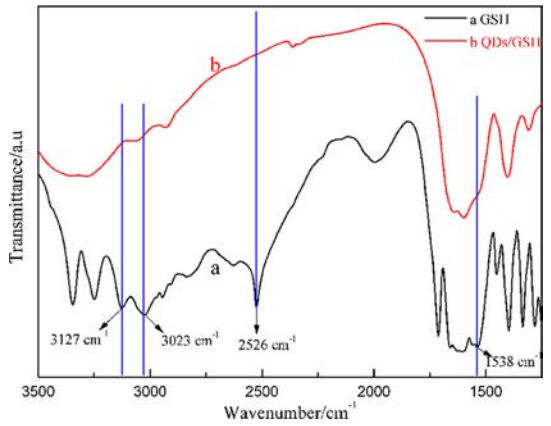

Figure 7. FTIR spectra of (a) free GSH and (b) GSH-capped CdTe:Zn^{2+} QDs.

ance of the N−H stretching bands, and the weakening of the amide bond clearly indicates that GSH may combine onto the surface of the QDs through the −SH and −NHR groups.[42]

The cytotoxicity of QDs is a critical characteristic for future biological applications, especially applications in cellular as well as in vivo imaging. In this work, the cytotoxicity of GSH-capped CdTe:Zn^{2+} QDs was evaluated by a microcalorimetric technique. Furthermore, for comparison, the MPA-capped CdTe QDs[22] was also studied with the same method.

The metabolism thermogenic curve of *Tetrahymena* in the medium as a control group without QDs at 28 °C is shown in Figure 8 (curve 1), which is consistent with the previous

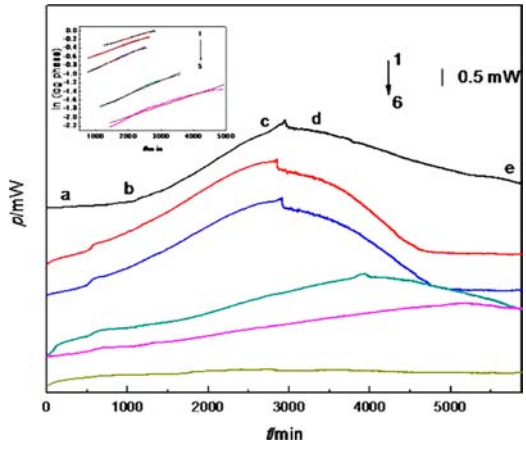

Figure 8. Growth thermogenic curves of *Tetrahymena* affected by GSH-capped CdTe:Zn^{2+} QDs at 28 °C: 1, 0; 2, 10 × 10^{-8}; 3, 20 × 10^{-8}; 4, 60 × 10^{-8}; 5, 80 × 10^{-8}; and 6, 100 × 10^{-8} mol/L (the inset is the exponential fitting curves).

reports (four phases, a lag phase (points a and b), a log (exponential) phase (points b and c), a stationary phase (points c and d), and a decline phase (points d and e)),[24] and the thermogenic curves of *Tetrahymena* growth affected by different concentrations of GSH-capped CdTe:Zn^{2+} QDs are also shown in Figure 8 (curves 2−6) (the data of MPA-capped CdTe QDs are not shown).

The growth thermogenic curves of the log phase correspond to eq 1:[24]

$$p_t = p_0 \exp(kt)$$

dx.doi.org/10.1021/ic300473u | *Inorg. Chem.* 2012, 51, 9208−9213

or

$$\ln P_t = \ln P_0 + kt \quad (1)$$

where k represents the metabolism rate constant or growth rate constant and P_0 and P_t are the heat output power of the microorganism (*Tetrahymena*) at times 0 and t (min), respectively. The time points for all curves are chosen from the beginning to the end of the log phase. The linear correlation coefficients are ≥0.9900.

The power−time curves were recorded for different concentration QDs as shown in Figure 8. These curves describe the evolution of the thermal effect of *Tetrahymena*. When the nutrition in the culture was used up, *Tetrahymena* cell will die consequently. Therefore, the metabolism would stop and the thermal effect disappeared (points c and d). With the concentration increasing, the growth rate of *Tetrahymena* reduced and the maximum of the power output changed in a regular fashion, indicating prolongation or inhibition of the whole metabolic process. The relationship between growth rate constant (k) and concentration of QDs (C) is shown in Table 2. From Table 2, it can be concluded that k decreases obviously

Table 2. Values of k, I, and IC_{50} of *Tetrahymena* in Different QDs at 28.0 °C

QDs	$c/10^{-8}$ M	k/min^{-1}	I/%	IC_{50}/M
GSH-capped CdTe:Zn^{2+}	0	0.00139	0	38.00×10^{-8}
	10	0.00111	22.07	
	20	0.00106	25.18	
	60	4.91×10^{-4}	67.34	
	80	3.93×10^{-4}	79.71	
	100	0	100	
GSH-capped CdTe	0	0.00135	0	18.88×10^{-8}
	5	0.00128	5.19	
	10	0.00125	7.4	
	15	0.00113	16.3	
	20	5.48×10^{-4}	59.4	
	30	4.61×10^{-4}	65.9	
	40	3.85×10^{-4}	71.5	
MPA-capped CdTe	0	0.00133	0	10.09×10^{-8}
	1	0.00125	10.07	
	2	0.00164	100.18	
	5	8.09×10^{-4}	41.78	
	7	7.25×10^{-4}	47.86	
	10	7.16×10^{-4}	48.46	
	20	3.00×10^{-4}	78.42	
	25	2.10×10^{-4}	84.88	

with increasing concentration of QDs. The almost complete inhibition of *Tetrahymena* activity was observed when k is close to zero.

The inhibitory ratio is defined as

$$I = \frac{k_0 - k_c}{k_0} \times 100\% \quad (2)$$

In eq 2, k_c and k_0 are the growth rate constants in the presence or absence of complexes, respectively. The results of I are also shown in Table 2. When the inhibitory ratio is 50%, the concentration of QDs is defined as half inhibition concentration (IC_{50}). In another word, the smaller the inhibitory ratio is, the more toxic the complex is. According to the relationship between k and c, the values of IC_{50} are obtained as shown in Table 2. The results of IC_{50} show that the GSH-capped CdTe QDs exhibit stronger toxicity (about 2 times) than GSH-capped CdTe:Zn^{2+} QDs. The microcalorimetric test suggests the addition of Zn ions, and the epitaxial growth of a CdS layer reduces the cytotoxicity of QDs to a significant extent. The toxicity of MPA-capped CdTe was also considered, indicating the formation of a CdS shell with GSH. As we know, the cytotoxicity of CdTe QDs is believed to arise from the released toxic metal ion Cd^{2+}.[43] So the Cd^{2+} released from QDs (GSH-capped CdTe:Zn^{2+}, GSH-capped CdTe, and MPA-capped CdTe) have been detected by ICP-AES. The results listed in Table 3 show the amount of released Cd^{2+} is correlated with

Table 3. Concentration of Cd^{2+} Released from Different QDs

quantum dots	QDs (mol/L)	Cd^{2+}(mg/L, supernatant)
GSH-capped CdTe: Zn^{2+}	10^{-5}	0.010 ± 0.006
GSH-capped CdTe	10^{-5}	0.019 ± 0.015
MPA-capped CdTe	10^{-5}	0.032 ± 0.004

the kind of QDs. It is evident that GSH-capped CdTe:Zn^{2+} QDs are the lowest toxicity and also suggest the most stability. This is because that Zn ions can also prevent the leaking of Cd ions.

CONCLUSIONS

By using GSH as a stabilizer and Zn ions as a dopant, high-quality water-soluble GSH-capped CdTe:Zn^{2+} QDs have been successfully synthesized through a one-step method in this work. Thanks to the existence of Zn ions and formation of a protective CdS shell on the CdTe core, our as-prepared QDs exhibit low cytotoxicity by the microcalorimetric technique and ICP-AES. The properties and structure of QDs are characterized by absorption, FL spectra, TEM, XRD, XPS, EDS, and FTIR. The QDs synthesized in this work will be promising nanomaterials as fluorescent labels for bioapplications.

AUTHOR INFORMATION

Corresponding Author

*Fax: +86 27 87863157. Phone: +86 27 87756779. E-mail: wangqisui520@163.com.

Notes

The authors declare no competing financial interest.

ACKNOWLEDGMENTS

We gratefully acknowledge the financial support by the Fundamental Research Funds for the Central Universities (Grant 2011-Ia-035), the National Natural Science Foundation of China (Grant No. 51175394), and the China Scholarship Council. The authors thank MissYe Chen for her help and useful discussions.

REFERENCES

(1) Resch, U.; Weller, H.; Henglein, A. *Langmuir* **1989**, *5*, 1015.
(2) Alivisatos, A. P. *J. Phys. Chem. B* **1996**, *100*, 13226.
(3) Kagan, C. R.; Murray, C. B.; Bawendi, M. G. *Phys. Rev. B: Condens. Matter* **1996**, *54*, 8633.
(4) Nirmal, M.; Brus, L. *Acc. Chem. Res.* **1999**, *32*, 407.
(5) Liu, P.; Duan, W.; Wang, Q.; Li, X. *Colloid Surf. B* **2010**, *78*, 171.
(6) Li, Y.; Jing, L.; Qiao, R.; Gao, M. *Chem. Commun.* **2011**, *47*, 9293.

(7) Gaponik, N.; Rogach, A. L. *Phys. Chem. Chem. Phys.* **2010**, *12*, 8685.
(8) Liu, Y. F.; Yu, J. S. *J. Colloid Interface Sci.* **2010**, *351*, 1.
(9) Li, W. W.; Liu, J.; Sun, K.; Dou, H. J.; Tao, K. *J. Mater. Chem* **2010**, *20*, 2133.
(10) Zhao, D.; He, Z.; Chan, W. H.; Choi, M. M. F. *J. Phys. Chem. C* **2009**, *113*, 1293.
(11) Zhang, Y.; Li, Y.; Yan, X.-P. *Small* **2009**, *5*, 185.
(12) Zhou, Y. L.; Yang, M.; Sun, K.; Tang, Z. Y.; Kotov, N. A. *J. Am. Chem. Soc.* **2010**, *132*, 6006.
(13) Xing, M.; Shen, H.; Zhao, W.; Liu, Y.; Du, Y.; Yu, Z.; Chen, X. *Biotechniques* **2011**, *50*, 259.
(14) Xu, J.; Yang, X.; Wang, H.; Chen, X.; Luan, C.; Xu, Z.; Lu, Z.; Roy, V. A. L.; Zhang, W.; Lee, C.-S. *Nano Lett.* **2011**, *11*, 4138.
(15) Murray, C. B.; Norris, D. J.; Bawendi, M. G. *J. Am. Chem. Soc* **1993**, *115*, 8706.
(16) Viale, Y.; Gilliot, P.; Crégut, O.; Likforman, J.-P.; Gallart, M.; Hönerlage, B.; Mariette, H. *Phys. Rev. B* **2004**, *69*, 115324.
(17) DeGroot, M. W.; Rösner, H.; Corrigan, J. F. *Chem.—Eur. J.* **2006**, *12*, 1547.
(18) Law, W.-C.; Yong, K.-T.; Roy, I.; Ding, H.; Hu, R.; Zhao, W.; Prasad, P. N. *Small* **2009**, *5*, 1302.
(19) Zhao, D.; Fang, Y.; Wang, H.; He, Z. *J. Mater. Chem.* **2011**, *21*, 13365.
(20) Regulacio, M. D.; Han, M. Y. *Acc. Chem. Res.* **2010**, *43*, 621.
(21) Ge, C.; Xu, M.; Liu, J.; Lei, J.; Ju, H. *Chem. Commun.* **2008**, *4*, 450.
(22) Li, L.; Qian, H.; Fang, N.; Ren, J. *J. Lumin.* **2006**, *116*, 59.
(23) Peng, L.; Yi, L.; Zhexue, L.; Juncheng, Z.; Jiaxin, D.; Daiwen, P.; Ping, S.; Songsheng, Q. *J. Inorg. Biochem.* **2004**, *98*, 68.
(24) Peng, L.; Lifang, R.; Hongyu, X.; Xi, L.; Chaocan, Z. *Biol. Trace Elem. Res.* **2007**, *115*, 195.
(25) Fang, T.; Li, X.; Wang, C.; Zhang, Z.; Zhang, T.; Zeng, J.; Liu, P.; Zhang, C. *J. Therm. Anal. Calorim.* **2012**, *109*, 433.
(26) Bao, H. B.; Gong, Y. Y.; Zhen, L.; Gao, M. Y. *Chem. Mater.* **2004**, *16*, 3853.
(27) Borchert, H.; Talapin, D. V.; Gaponik, N.; McGinley, C.; Adam, S.; Lobo, A.; Moller, T.; Weller, H. *J. Phys. Chem. B* **2003**, *107*, 9662.
(28) Zhong, X. H.; Feng, Y. Y.; Knoll, W.; Han, M. Y. *J. Am. Chem. Soc.* **2003**, *125*, 13559.
(29) Zhong, X.; Han, M.; Dong, Z.; White, T. J.; Knoll, W. *J. Am. Chem. Soc.* **2003**, *125*, 8589.
(30) Zhong, X.; Liu, S.; Zhang, Z.; Li, L.; Wei, Z.; Knoll, W. *J. Mater. Chem* **2004**, *14*, 2790.
(31) Liu, F.-C.; Cheng, T.-L.; Shen, C.-C.; Tseng, W.-L.; Chiang, M. Y. *Langmuir* **2008**, *24*, 2162.
(32) Wang, Y.; Hou, Y.; Tang, A.; Feng, B.; Li, Y.; Liu, J.; Teng, F. *J. Cryst. Growth* **2007**, *308*, 19.
(33) Henglein, A. *Chem. Rev.* **1989**, *89*, 1861.
(34) Gattas-Asfura, M. K.; Leblanc, R. M. *Chem. Commun.* **2003**, 2684.
(35) Qian, H.; Dong, C.; Weng, J.; Ren, J. *Small* **2006**, *2*, 747.
(36) Sheng, Z.; Han, H.; Hu, X.; Chi, C. *Dalton Trans* **2010**, *39*, 7017.
(37) Yu, W. W.; Qu, L.; Guo, W.; Peng, X. *Chem. Mater.* **2003**, *15*, 2854.
(38) Chen, L.-N.; Wang, J.; Li, W.-T.; Han, H.-Y. *Chem Comm* **2012**, *48*, 4971.
(39) Mekis, I.; Talapin, D. V.; Kornowski, A.; Haase, M.; Weller, H. *J. Phys. Chem. B* **2003**, *107*, 7454.
(40) Smith, A. M.; Mohs, A. M.; Nie, S. *Nat. Nanotechnol.* **2009**, *4*, 56.
(41) Deng, Z.; Schulz, O.; Lin, S.; Ding, B.; Liu, X.; Wei, X.; Ros, R.; Yan, H.; Liu, Y. *J. Am. Chem. Soc.* **2010**, *132*, 5592.
(42) Zhang, J.; Li, J.; Zhang, J.; Xie, R.; Yang, W. *J. Phys. Chem. C* **2010**, *114*, 11087.
(43) Su, Y.; Hu, M.; Fan, C.; He, Y.; Li, Q.; Li, W.; Wang, L.; Shen, P.; Huang, Q. *Biomaterials* **2010**, *31*, 4829.